

## SUPPORTING INFORMATION

### **The Effect of Physical Morphology of Dried Biofluids on Chemical Stability of Analytes Stored in Paper and Direct Analysis by Mass Spectrometry**

Benjamin S. Frey,<sup>a</sup> Deidre E. Damon,<sup>a</sup> and Abraham K. Badu-Tawiah\*<sup>a</sup>

<sup>a</sup>Department of Chemistry and Biochemistry, The Ohio State University, Columbus, OH 43210

\*Corresponding Author:

Prof. Abraham Badu-Tawiah:

Tel.: (614) 929-4276

Email: [badu-tawiah.1@osu.edu](mailto:badu-tawiah.1@osu.edu)

Supporting information is summarized below:

## Table of Contents

	Description	Page
	<u>Experimental Methods</u>	S3
	<u>Results and Discussion</u>	
	<b><i>Chemical Changes Observed in Cracked Dried Blood Spheroids</i></b>	
Fig. S1	Stability plot of cocaine-spiked dried blood spheroid that has dried and cracked under uncontrolled ambient storage conditions	S4
	<b><i>Application of Exogenous Polymer Coating to Dried Matrix Spots on Paper</i></b>	
Fig. S2	Drop-casting methodology for application of xanthan gum polymer to sample	S5
	<b><i>Impact of Exogenous Polymer on Sample Integrity</i></b>	
Fig. S3	Micrographs of surface morphology of xanthan-gum coated dried blood spots and dried blood spheroids	S6
Fig. S4	Micrograph of the mixing process of polymer with a dried methylene blue sample spot on hydrophobic paper	S7
Fig. S5	Micrographs of xanthan-gum coated dried blood spots and dried blood spheroids	S8
Fig. S6	Micrographs of xanthan-gum infused dried blood spots and dried blood spheroids	S9
Fig. S7	Micrographs of dried blood spots and dried blood spheroids diluted with xanthan gum solution	S10
Fig. S8	Focused ion beam micrographs of the superficial polymer layer of a xanthan gum-coated dried blood spot	S11

## ***Mass Spectra of Performance Enhancing Drugs Spiked in Urine***

Table S1	Precision measurements for all stability experiments performed pertaining to cocaine in whole blood and clenbuterol and trenbolone in urine	S12
Fig. S9	Full MS spectra for clenbuterol and trenbolone spiked in urine on hydrophilic paper substrate without xanthan gum treatment	S13
Fig. S10	MS/MS spectra for clenbuterol and trenbolone spiked in urine on hydrophilic paper substrate with xanthan gum treatment	S14
<b><i>Relative Ionization Efficiency of Polymer-coated Dried Sample Spots on Paper</i></b>		
Fig. S11	Relative Ionization Efficiency curves for performance enhancing drugs in dried urine spots	S15
Table S2	Percent difference of relative ionization efficiency curves for xanthan gum-coated samples on hydrophilic and hydrophobic paper substrates	S16
<b><i>Matrix Effects of Dried Urine Spots on Paper Substrate</i></b>		
Table S3	Matrix effects of dried urine spots with and without xanthan gum coating on hydrophilic and hydrophobic paper substrates	S17
	References	S17

## Experimental Methods

### Humidity-controlled stored samples

To create high and low humidity conditions in humidity-controlled sample storage containers, 15 g and 100 g of potassium hydroxide pellets (ACS grade) were dissolved in 200 mL of nanopure water for final concentrations of 1.33 M and 8.91 M, respectively. To estimate the percent relative humidity, a set of hydrometers were used to measure the specific gravity of the solution in accordance to the literature.<sup>1,2</sup>

Home-built humidity chambers were created by adding 100 mL of dilute potassium hydroxide solution to a pipette tip box. After addition of the solution, hydrophobic squares or triangles were placed on top of the tip tray. 4 or 10  $\mu$ L of whole blood was then deposited on the paper substrate. The humidity chambers were then sealed off using parafilm until photography or analysis was performed. For stability and drying studies, the samples were re-sealed immediately after photography or analysis steps unless stated otherwise.

### Scanning Electron Microscopy (SEM) and Focused Ion Beam Microscopy (FIB)

Dried biofluid samples (blood, plasma, serum) on paper squares were fixed in 2.5% glutaraldehyde in 0.1 M phosphate buffer pH 7.4 for a minimum of 72 hours. Samples were then rinsed 2  $\times$  5 minutes with 1XPBS and then 2  $\times$  5 minutes in water. Samples were then allowed to dry overnight in ambient air and sputter coated with a thin layer of AuPd or Au. The samples analyzed for thin film thickness were analyzed without any metal coating at room temperature with a water vapor pressure of 50 Pa in the chamber. A FEI Nova 400 NanoSEM, Thermo Scientific Apreo LoVac Analytical SEM, and Nova NanoLab 600 DualBeam FIB were used to collect images. ImageJ software was utilized to measure thin film thickness.

## Results and Discussion

### Chemical Changes Observed in Cracked Dried Blood Spheroids

To determine the impact of artifacts in structural morphology such as cracking/cratering in dried blood spheroids on chemical stability, the signal for cocaine was monitored in dried blood spheroids under un-regulated ambient storage conditions for 0, 1, 2, 5, 7, and 10 days. The resulting dried blood spheroids were analyzed using PS-MS and the data was normalized to data derived from day zero. Cocaine was found to rapidly degrade in cracked spheroids which is not observed for in-tact spheroids without cracks or cratering. This cracking is detrimental to the protective mechanism of dried blood spheroids that provides enhanced stability to labile analytes stored within the interior bulk. For example, direct paper spray analysis of cracked dried blood spheroids (i.e., samples in Figure 1B, i) that were dried in ambient air showed a marked difference in analyte stability (Figure S1) when

compared to a typical dried blood spheroid (i.e., samples in Figure 1B, ii and corresponding stability data is shown in Figure 2A). Cracking of 3D structures and thin films exposes the interior bulk to environmental stressors at a more rapid rate, resulting in more rapid degradation of stored molecules. Other factors have previously been shown to increase the rate of chemical decomposition, such as the formation of oxygen adducts in sample.<sup>3</sup>

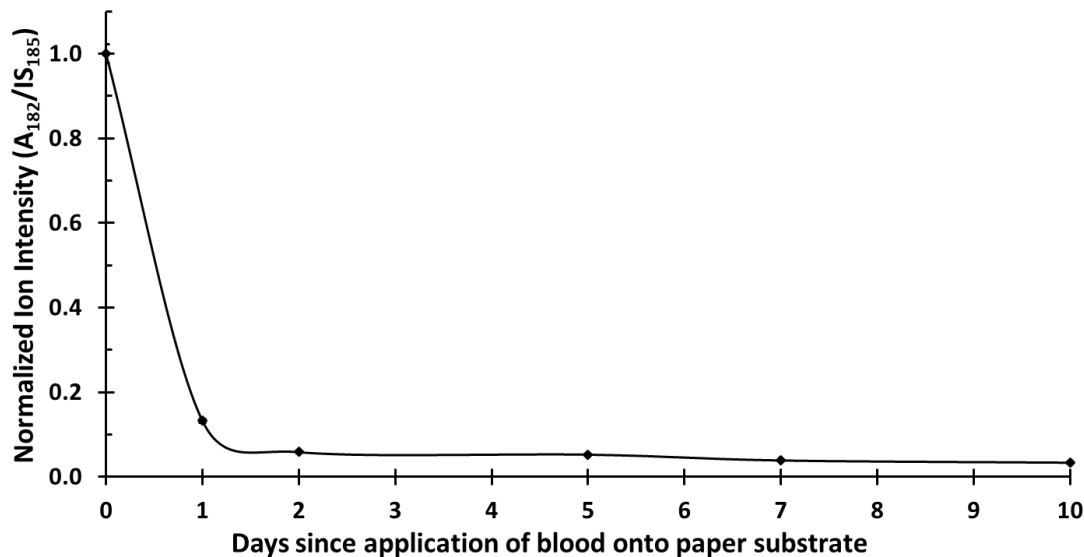


**Figure S1.** Stability diagram for cocaine-spiked whole blood (10  $\mu$ L) on hydrophobic paper substrate. Analyte signal (cocaine;  $m/z$  304  $\rightarrow$  182) was measured for each day relative to the signal derived from internal standard (cocaine-d3;  $m/z$  307  $\rightarrow$  185).

### Drop-casting methodology for application of xanthan gum polymer to sample

The concentration of (5 mg/mL) of xanthan gum polymer solution used in this work was close to the point of saturation. We opted for a larger concentration to guarantee that the sample would be sufficiently treated. This decision was guided by looking for concentration which resulted in a much more viscous solution and still did not cause the spheroids to “crash out” and increase their surface area. Such an effect will potentially interrupt the formation of the protective barrier we need.

The process of coating dried biofluid samples with xanthan gum polymer is summarized in **Figure S2** below. The biofluid sample is first deposited onto paper substrate and is air-dried for 2 h at room temperature. The resulting dried matrix spot is then coated with an aliquot of xanthan gum polymer via drop-casting with a pipette, using a circular motion to encapsulate the sample, which is subsequently re-dried under ambient conditions for 2 h before direct analysis via paper spray mass spectrometry. The volume of xanthan gum solution is at least 1.2X that of the original sample spot volume.

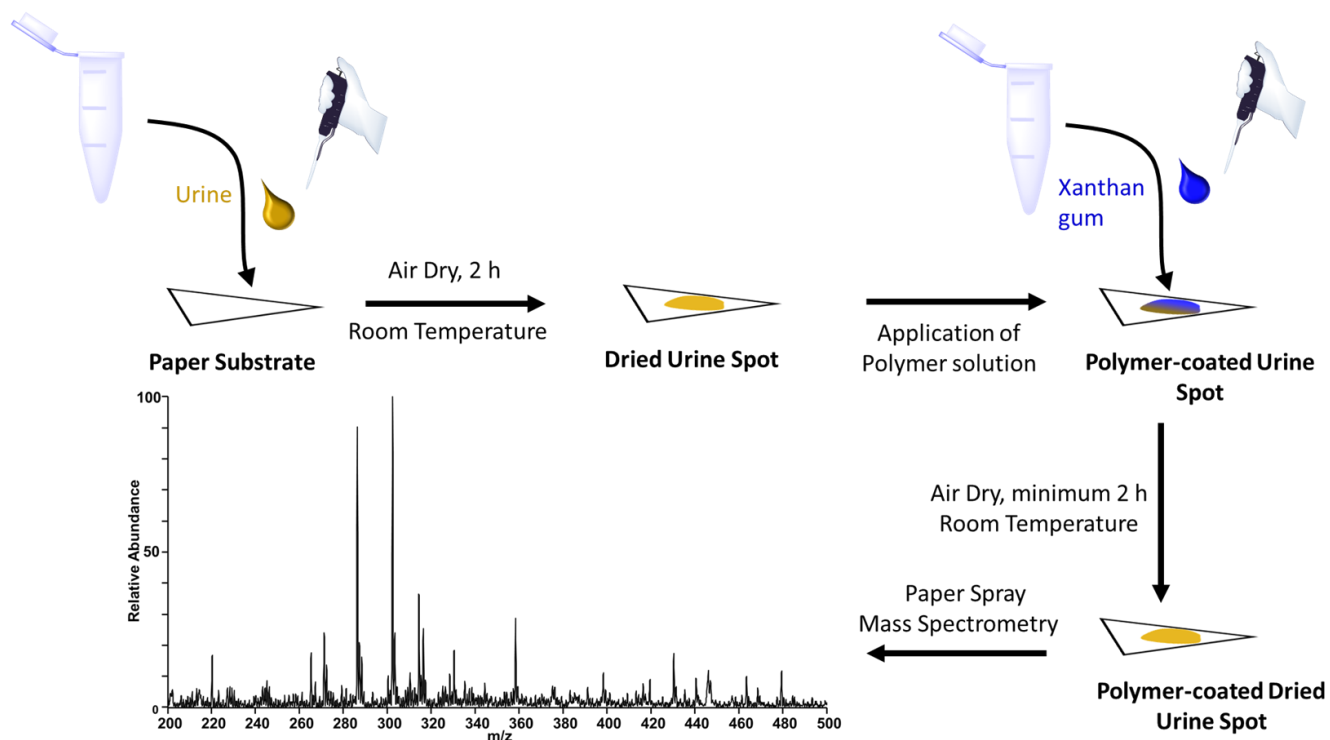


**Figure S2.** Drop-casting methodology for the application of xanthan gum polymer to dried matrix spots on paper substrate.

### Impact of Exogenous Polymer on Sample Integrity

To investigate the impact of exogenous polymer on the sample integrity, 10  $\mu\text{L}$  dried blood spots (DBS) and dried blood spheroids were imaged through compound light microscopy and scanning electron microscopy (SEM). Xanthan gum polymer was used to treat the samples using three different methodologies: (1) direct coating of an air-dried matrix spot with polymer solution, (2) direct infusion of polymer solution into a freshly deposited matrix spot, and (3) direct dilution of biofluid matrix with polymer solution prior to spotting sample onto paper substrates. The matrix spots were subsequently imaged after being treated with polymer solution and air-dried under ambient conditions. Morphological surface features were observed for each type of application methodology, taking care to note the impact of polymer on red blood cell (RBC) morphology. The coating methodology yielded the best results with minimal sample preparation. The resulting coated dried matrix spots had an increased surface area compared to their non-coated counterparts (**Figures S3, S5, S6, and S7**).

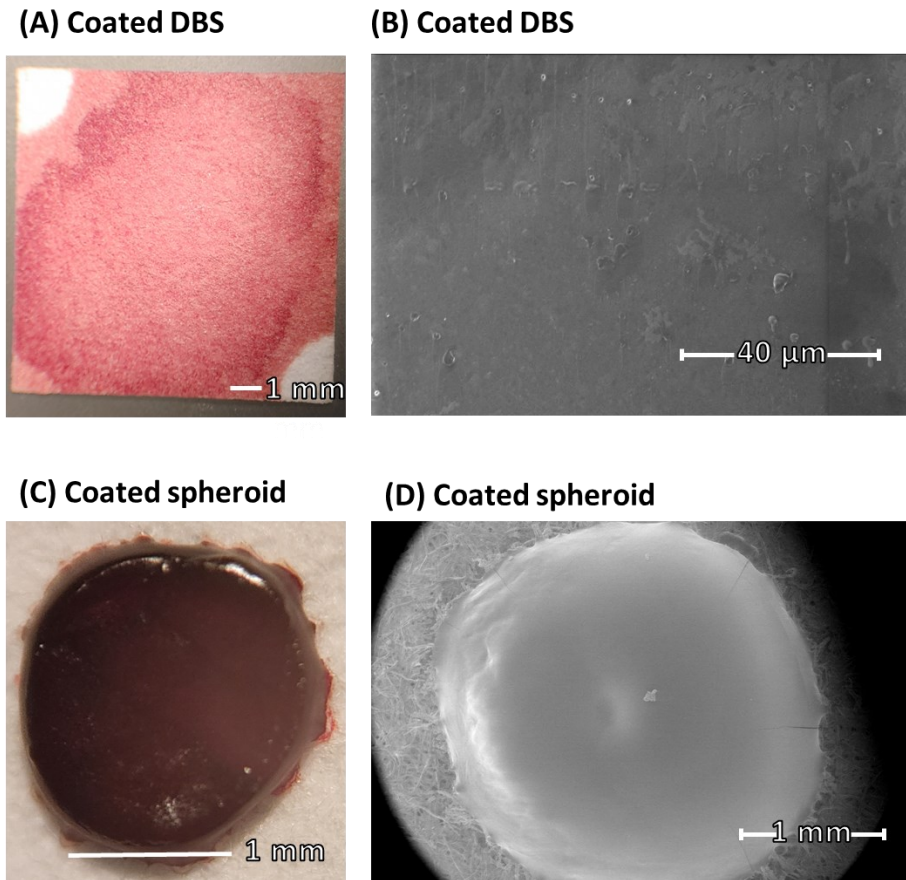
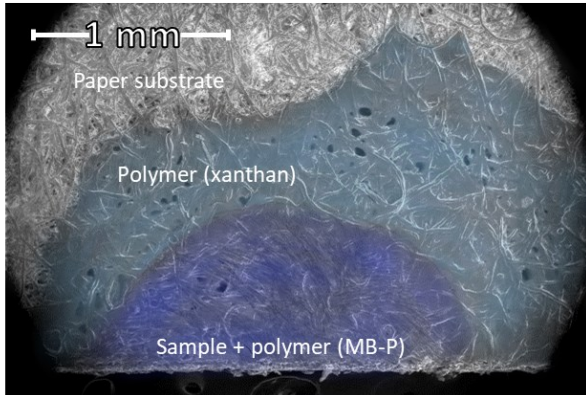


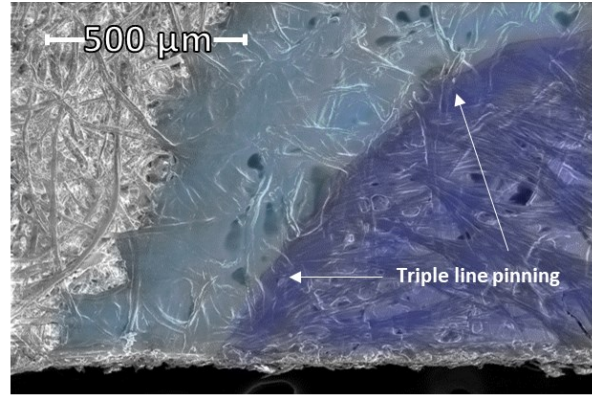
**Figure S3.** (A) Compound light micrograph of a 10  $\mu\text{L}$  polymer-coated DBS on hydrophilic paper. The sample undergoes concomitant mixing with the polymer solution and subsequently re-wets the paper substrate with a greater surface area. (B) SEM image of a 10  $\mu\text{L}$  polymer-coated DBS on hydrophilic paper. (C) Compound light micrograph of a 10  $\mu\text{L}$  polymer-coated dried blood spheroid on hydrophobic paper. The resulting spheroids dry with a significant reduction in cracking and cratering. (D) SEM image of a 10  $\mu\text{L}$  polymer-coated dried blood spheroid on hydrophobic paper.

The process of polymer solution mixing with sample was first investigated using methylene blue dye (MB) as a model system. In this experiment, 10  $\mu\text{L}$  of methylene blue dye was deposited onto hydrophobic paper substrate and air-dried under ambient conditions for 2 h. Polymer solution was then applied directly on top of the sample which was subsequently re-dried under ambient conditions for 2 h. The sample was then imaged using SEM. After the MB sample is initially deposited on the paper substrate, triple line pinning occurs, where the sample becomes immobilized; the hydrophobic-nature of the paper causes the sample to dry as a thin 2D biofilm on top of the paper substrate. When an aliquot of polymer solution is applied on top of the sample, the sample begins to resolubilize while the polymer solution begins to spread across the paper substrate over time. This process causes the resulting sample spot to have a greater surface area once dried. The original sample spot was found to be intact where the triple line can be visibly observed. A new sample spot boundary can be observed where polymer solution has wet the paper substrate (**Figure S4**).

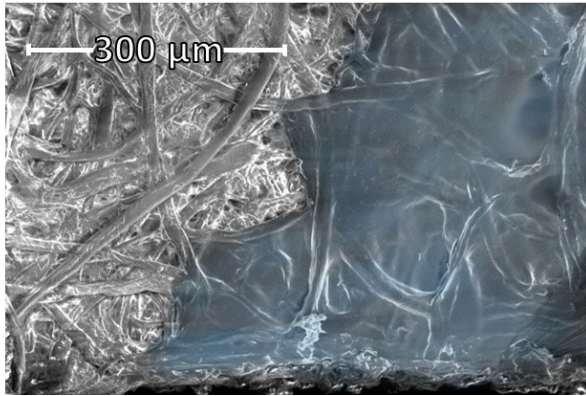
**(A) Top-down overview**



**(B) MB-P – xanthan – paper interfaces**



**(C) Xanthan – paper interface**



**(D) MB-P – xanthan interface**

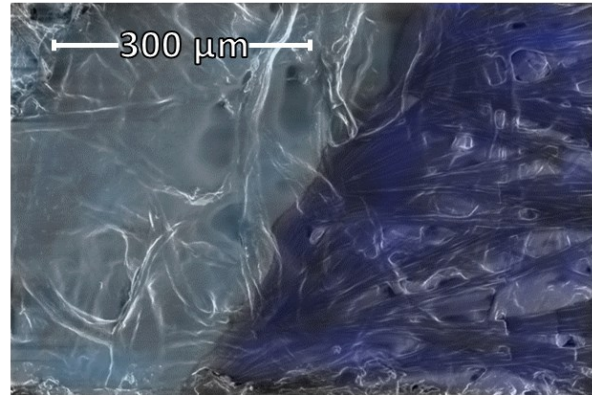


**Figure S4.** (A) Top-down view of a 10  $\mu\text{L}$  polymer-coated dried methylene blue spot on hydrophobic paper substrate. Two distinct interfaces can be observed: the paper-polymer interface (gray/light blue) and the polymer-sample interface (light blue/dark blue). The image has been modified with translucent blue filters for ease of viewing. (B) Zoomed-in view of the MB-polymer-paper interface showing triple line pinning. The original sample remains in place while the polymer solution wets a greater distance, resulting in the sample spot having a greater surface area relative to the non-coated sample. (C) Zoomed-in view of the MB-polymer interface.

The first polymer application methodology utilized was direct coating of dried biofluid matrix. The process described above was followed for these samples. Whole blood (10  $\mu\text{L}$ ) was first deposited onto hydrophilic and hydrophobic paper substrates. The samples were then air-dried for 2 h. Next, an aliquot of polymer solution was added atop the sample in a circular motion and samples were subsequently re-dried under ambient conditions. The samples were then imaged using compound light microscopy and SEM.



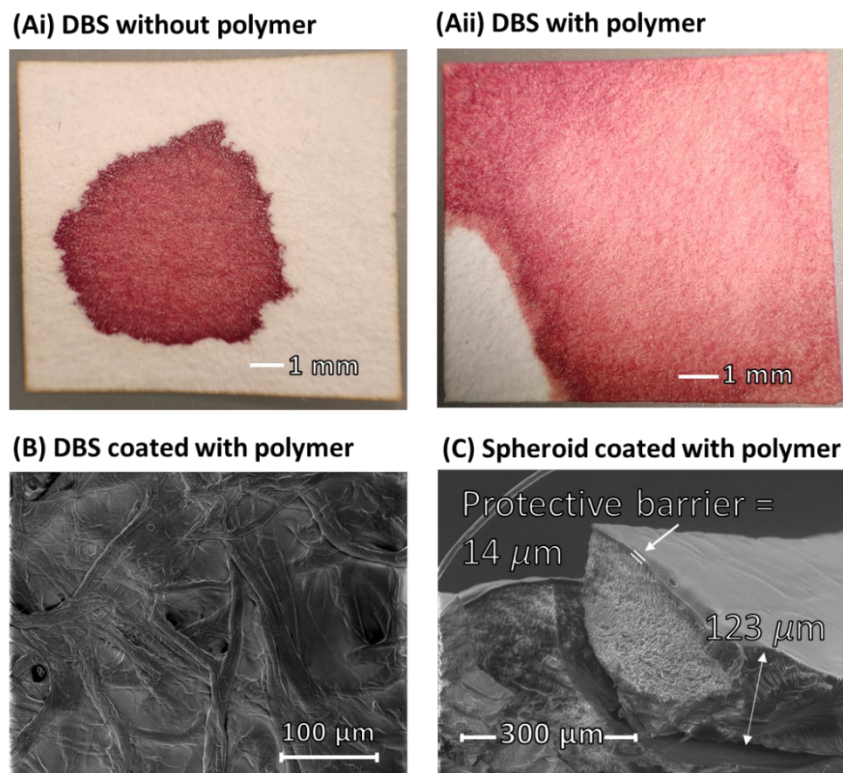


**Figure S5.** (Ai) Compound light micrograph of a conventional DBS on hydrophilic paper substrate. (Aii) Compound light micrograph of a polymer-coated DBS on hydrophilic paper substrate. The coated sample has a much larger surface area compared to the non-coated counterpart. There is a light void in the center where the original sample spot was deposited. (B) SEM image of 10  $\mu\text{L}$  polymer-coated DBS on hydrophilic paper. (C) SEM cross-sectional image of a 10  $\mu\text{L}$  polymer-coated dried blood spheroid on hydrophobic paper. The thin film thickness of the spheroid is much lower than that of the non-coated counterpart. The protective barrier of the spheroid still remains in-tact after application of polymer, with in-tact RBCs within the interior bulk of the spheroid showing that the polymer solution does not have a negative impact on the RBC morphology or natural drying process of the whole blood sample.

The second polymer application methodology utilized was direct infusion of polymer into a freshly deposited biofluid sample. Whole blood (5  $\mu\text{L}$ ) was first deposited onto hydrophilic and hydrophobic paper substrates. Next, 5  $\mu\text{L}$  of polymer solution was directly added to the freshly deposited sample. The samples were then allowed to dry under ambient conditions for 2 h. The samples were subsequently imaged using compound light microscopy and SEM. The polymer solution did not fully mix before the sample completely dried, resulting in patchy regions of polymer throughout the samples. This process was not adopted for further studies due to the inhomogeneity of polymer. The wetting process of polymer was also impacted by the presence of wet whole blood on the paper substrate. This is likely because the blood has already wicked through the paper substrate and the flow rate near the center is markedly reduced compared to the outer peripheral edges. This noticeable difference, compared to the coating process, is observed in **Figure S7A**.

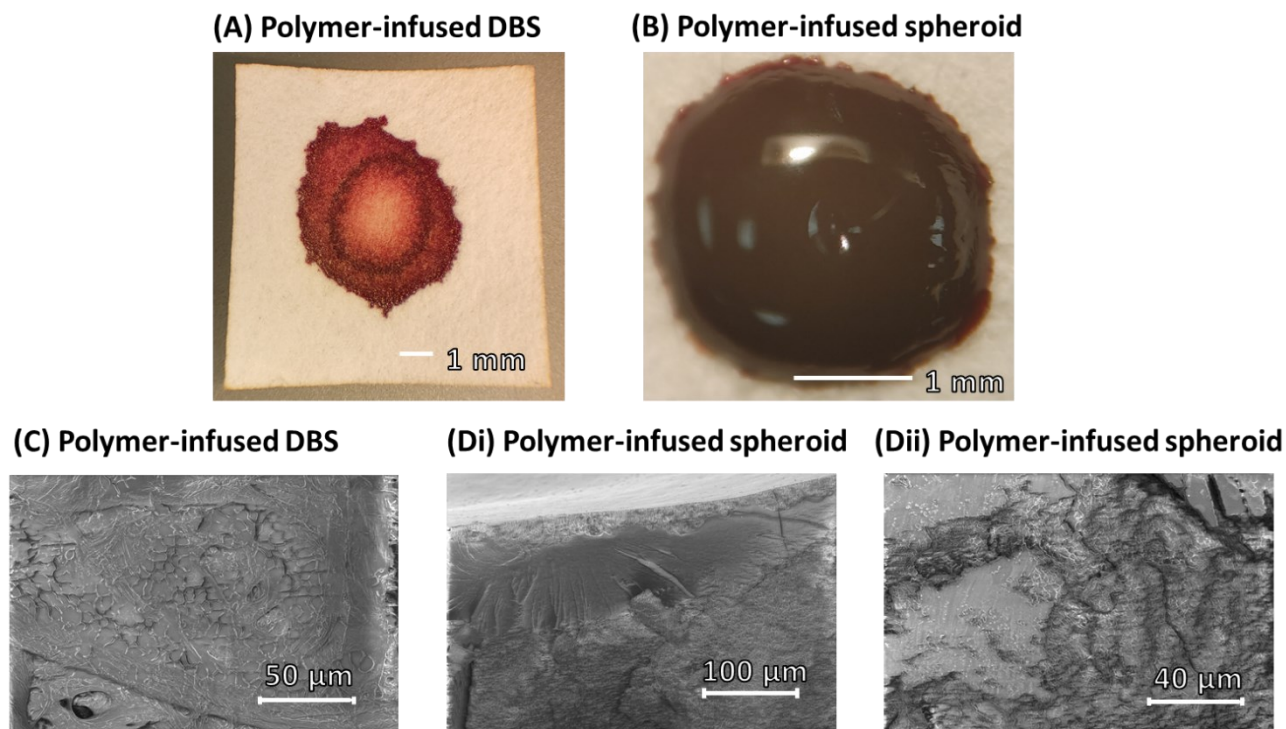


**Figure S6.** (A) Compound light micrograph of a 10  $\mu\text{L}$  polymer-infused DBS on hydrophilic paper. The polymer solution does not fully wet the sample and is confined towards the center. (B) Compound light micrograph of a 10  $\mu\text{L}$  polymer-infused dried blood spheroid on hydrophobic paper substrate. The resulting spheroid morphology is more round compared to non-coated dried blood spheroid samples which tend to have a more flat top surface. (C) SEM image of a 10  $\mu\text{L}$  polymer-infused DBS on hydrophilic paper. The polymer helps stabilize the sample; intact RBCs are observed within the pore of the paper substrate mixed with polymer solution. (Di) SEM cross-sectional image of a 10  $\mu\text{L}$  polymer-infused dried blood spheroid on hydrophobic paper. RBCs within the interior bulk of the spheroid remain in-tact with the formation of the natural protective barrier. (Dii) SEM cross-sectional image of a 10  $\mu\text{L}$  polymer-infused dried blood spheroid on hydrophobic paper. A patch of polymer solution can be observed and concentrated in a specific region of the spheroid (light gray area, has a higher density than blood).

The third polymer application methodology utilized was a direct dilution of whole blood with the polymer solution prior to spotting the samples onto paper substrate. Whole blood was first diluted with polymer solution (1:1, % v/v) and 10  $\mu\text{L}$  of sample was subsequently spotted onto hydrophilic and hydrophobic paper substrate. The samples were air-dried for 2 h prior to imaging with compound light microscopy and SEM. The polymer-diluted sample leads to a more controlled flow when deposited onto the paper substrate (**Figure S8A**) when compared to non-coated samples. While this approach yielded similar results to the coating methodology, the exact volume of biofluid sample must be known and deposited into a fresh sample requiring a pipette whereas the coating methodology is not volume-dependent and an inexpensive plastic bulb pipette can be used for application.

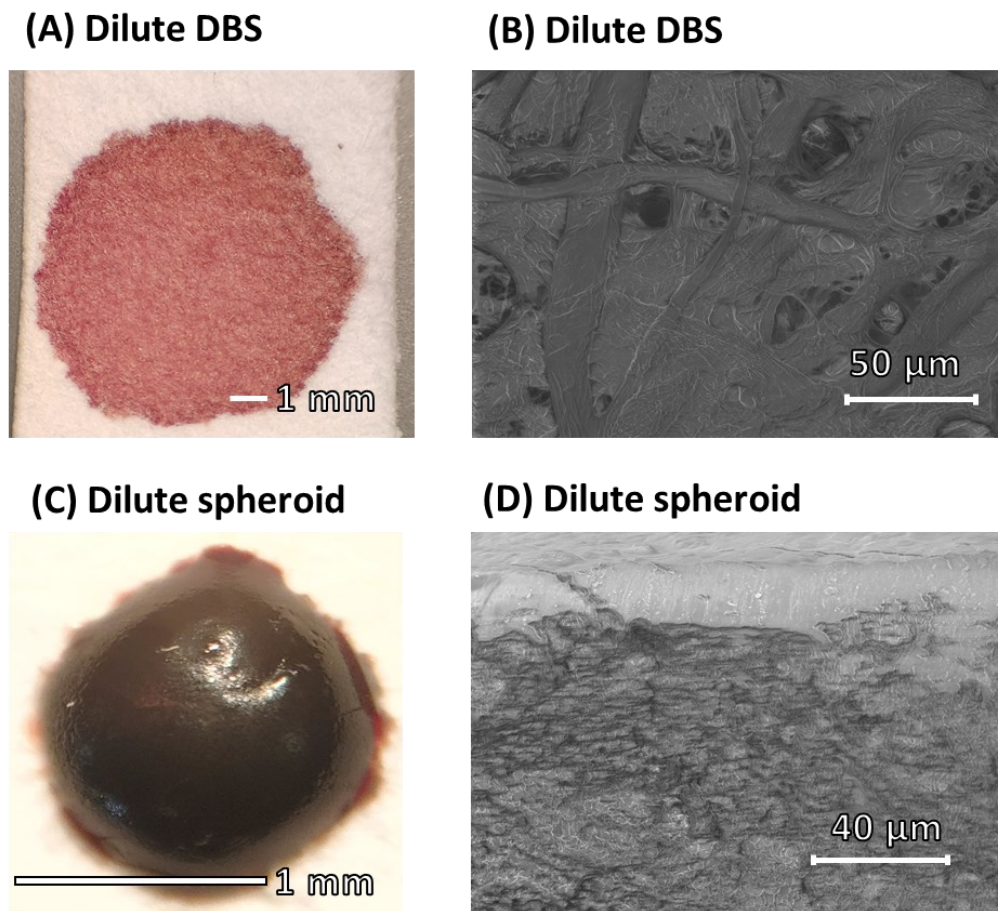
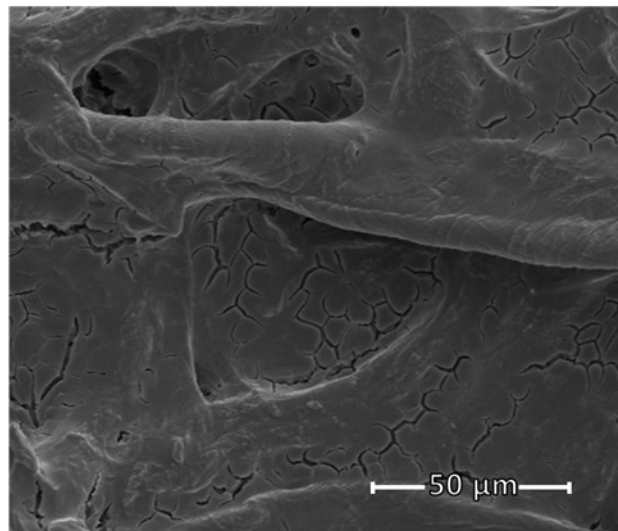


**Figure S7.** (A) Compound light micrograph of a 10  $\mu\text{L}$  DBS that has been diluted with polymer solution prior to spotting onto hydrophilic paper substrate. The resulting spot is more circular and has a more controlled flow compared to the non-coated DBS. (B) SEM image of a 10  $\mu\text{L}$  DBS that has been diluted with polymer solution prior to spotting onto hydrophilic paper substrate. (C) Compound light micrograph of a 10  $\mu\text{L}$  dried blood spheroid that has been diluted with polymer solution prior to spotting onto hydrophobic paper substrate. The surface morphology resembles that of the infused dried blood spheroid. (D) SEM cross-sectional image of a 10  $\mu\text{L}$  dried blood spheroid that has been diluted with polymer solution prior to spotting onto hydrophobic paper substrate. Due to mixing prior to spotting the sample, no patches of polymer were observed in the interior bulk like with the infused dried blood spheroid samples. Similar to the coated samples, the natural protective barrier still forms, and in-tact RBCs are observed in the interior bulk. The brightness was enhanced for this image by +20% for clarity.

To further characterize the artificial barrier, the superficial polymer layer on top of the paper substrate was imaged. Due to the viscous nature of the polymer solution, the polymer largely remains on the surface of the sample rather than being absorbed into the core of the paper substrate. This process was demonstrated using hydrophilic paper substrate. Whole blood (10  $\mu\text{L}$ ) was first diluted with polymer (1:1, % v/v) and subsequently deposited onto hydrophilic paper substrate and was air-dried for 2 h. The sample was then imaged using focused ion beam (FIB) microscopy (**Figure S8**).

**(A) Surface of coated DBS**



**(B) Polymer layer covering in-tact RBCs**

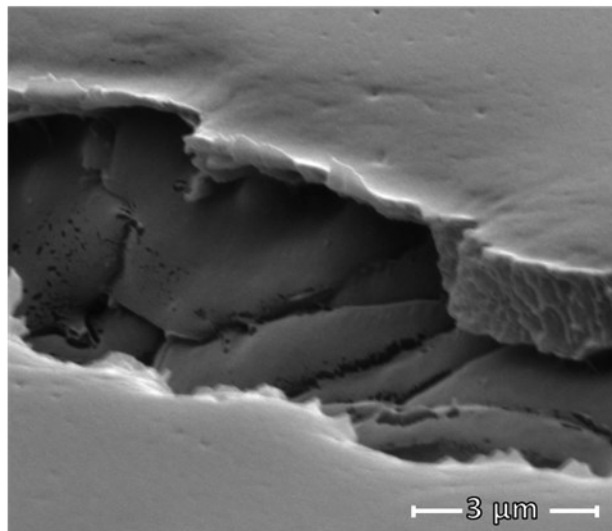


**Figure S8.** (A) FIB top-down view of a DBS diluted with polymer on hydrophilic paper substrate. In-tact RBCs under the thin polymer coating are observed. (B) FIB image of an artificial crack induced in the sample. The top layer comprises solely of polymer solution. Stacks of in-tact RBCs may be observed directly under the polymer layer. The polymer layer was measured to be 1.3  $\mu\text{m}$ .

### Precision Measurements Corresponding to Stability Experiments

Precision measurements corresponding to cocaine in whole blood and clenbuterol and trenbolone in urine have been provided below in Table S1 for all stability experiments performed.

**Table S1.** Precision measurements for cocaine-spiked whole blood and clenbuterol- and trenbolone-spiked urine with and without xanthan gum treatment on hydrophilic and hydrophobic paper substrates.

Analyte (matrix)	Paper Substrate	Polymer Treatment Method	RSD (%)	No. replicates
Cocaine (blood)	Hydrophilic	None (Control)	0.97 - 2.4	5
	Hydrophilic	Coated	0.72 - 1.82	5
	Hydrophilic	Infusion	0.47 - 1.99	5
	Hydrophilic	Dilution	0.31 - 2.58	5
	Hydrophobic	None (Control)	0.64 - 2.74	5
	Hydrophobic	Coated	0.15 - 3.39	5
	Hydrophobic	Infusion	0.20 - 4.48	5
	Hydrophobic	Dilution	0.50 - 2.47	5
Clenbuterol (urine)	Hydrophilic	None (Control)	0.43 - 8.04	3
	Hydrophilic	Coated	1.18 - 8.45	3
Trenbolone (urine)	Hydrophilic	None (Control)	0.92 - 9.15	3
	Hydrophilic	Coated	0.37 - 7.57	3

### Mass Spectra of Performance Enhancing Drugs Spiked in Urine

Full mass spectra were collected for clenbuterol- and trenbolone-spiked urine samples without xanthan gum treatment below in Figure S9. Tandem mass spectrometry (MS/MS) was performed on clenbuterol- and trenbolone-spiked urine samples spotted on hydrophilic paper substrates coated with polymer solution (Figure S10). The typical MS<sup>2</sup> transition for clenbuterol is  $m/z$  277 → 259 while the MS<sup>3</sup> transition for clenbuterol is  $m/z$  277 → 259 → 203. The typical MS<sup>2</sup> transition for trenbolone is  $m/z$  271 → 227.

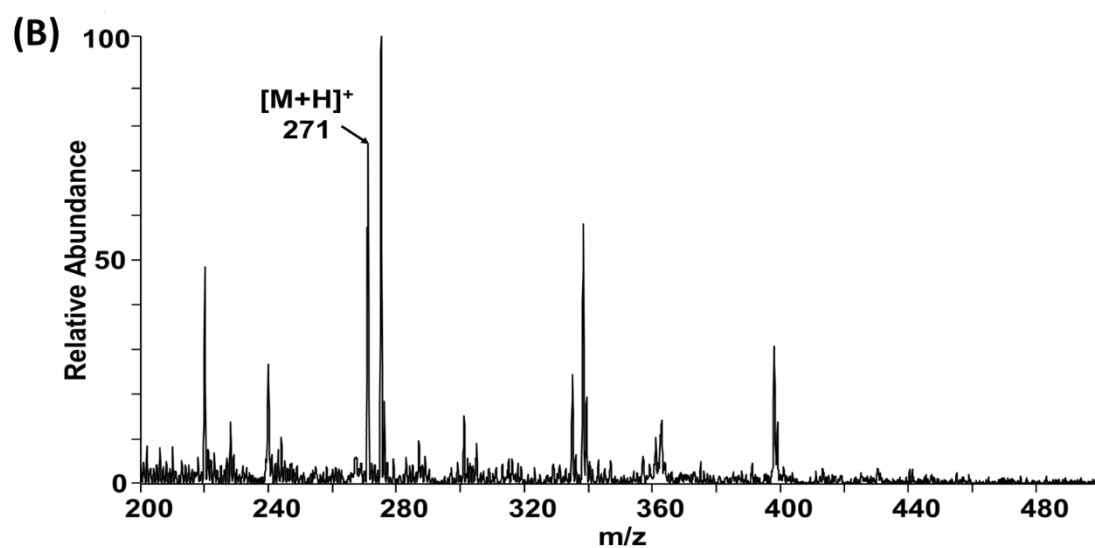
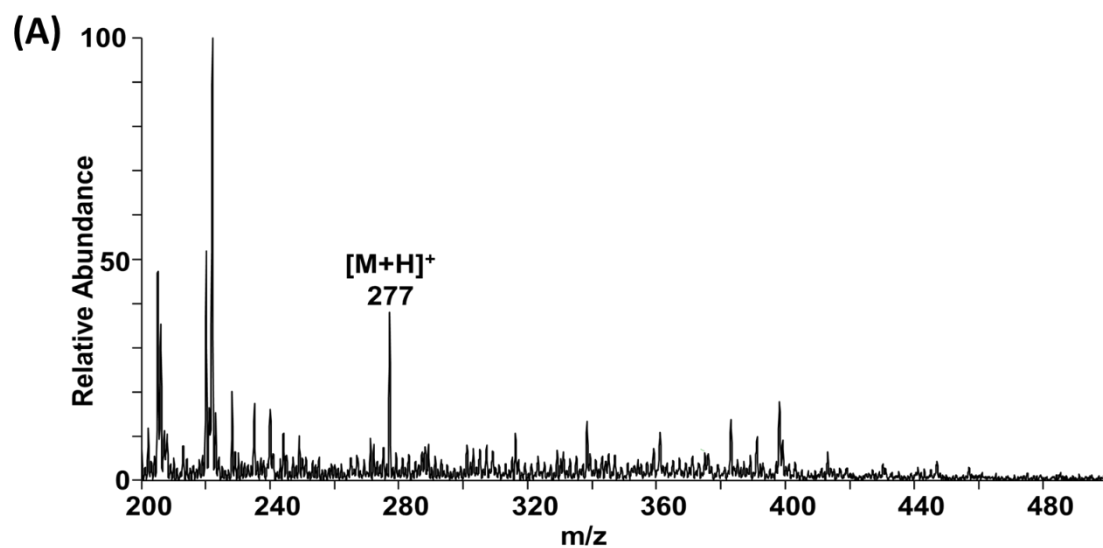


**Figure S9.** Full MS spectra of (A) clenbuterol ( $m/z$  277) and (B) trenbolone ( $m/z$  271) spiked in urine on hydrophilic paper substrate without xanthan gum treatment.

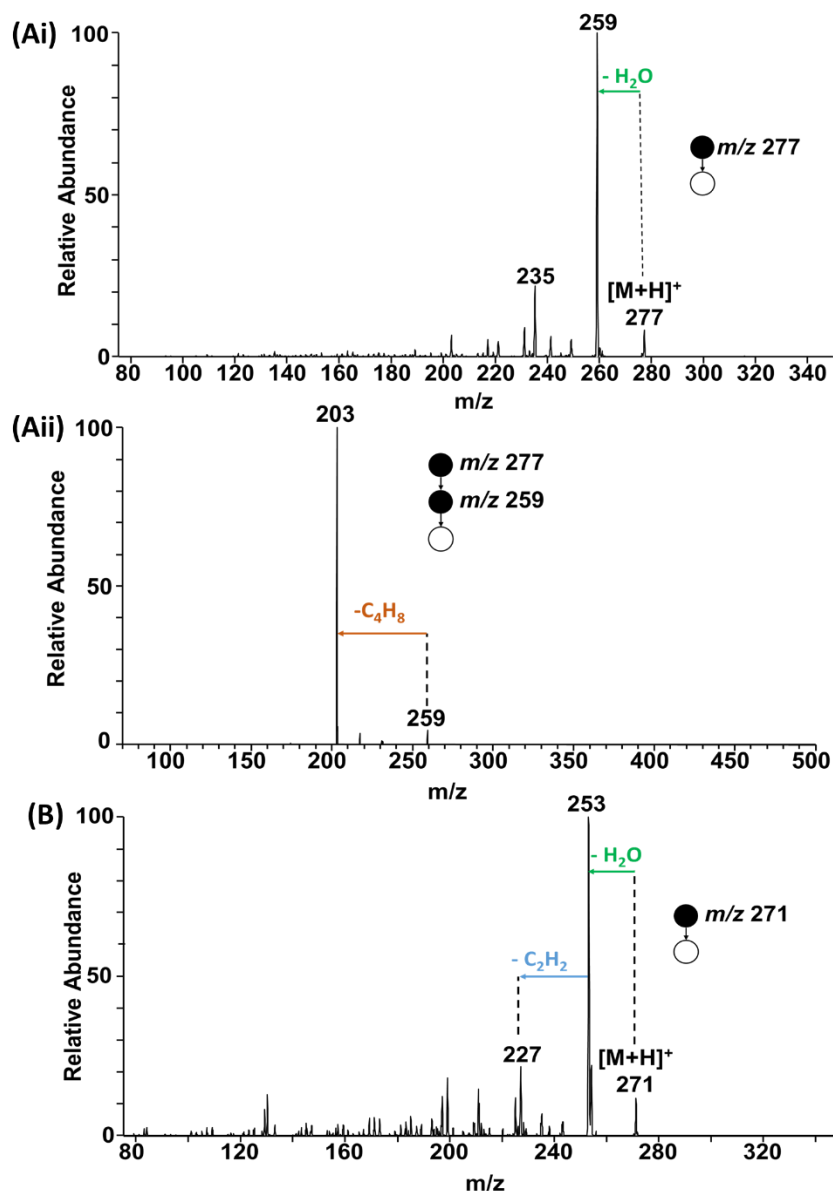


**Figure S10.** (Ai) MS<sup>2</sup> spectra for clenbuterol corresponding to the transition  $m/z$  277  $\rightarrow$  259. (Aii) MS<sup>3</sup> spectra for clenbuterol corresponding to the transition  $m/z$  277  $\rightarrow$  259  $\rightarrow$  203. (B) MS<sup>2</sup> spectra for trenbolone corresponding to the transition  $m/z$  271  $\rightarrow$  227.

### Relative Ionization Efficiency of Polymer-coated Drug Samples

To determine the impact of polymer coating on the analysis step, the relative ionization efficiency of performance enhancing drugs was monitored for dried matrix spots (DMS) on hydrophilic and hydrophobic paper substrates with and without polymer coating. The signal for analytes (A) clenbuterol and trenbolone were monitored relative to their internal standards (IS) clenbuterol-d<sub>9</sub> and nandrolone in MS/MS mode. All samples were extracted with ethyl acetate, 0.1% formic acid. From the linear response of the generated curves, the slope,  $m$ , was obtained,

where  $m \times 100$  corresponds to the relative ionization efficiency (%). The correlation coefficient (R2) for each curve was determined to be  $\geq 0.9987$ .

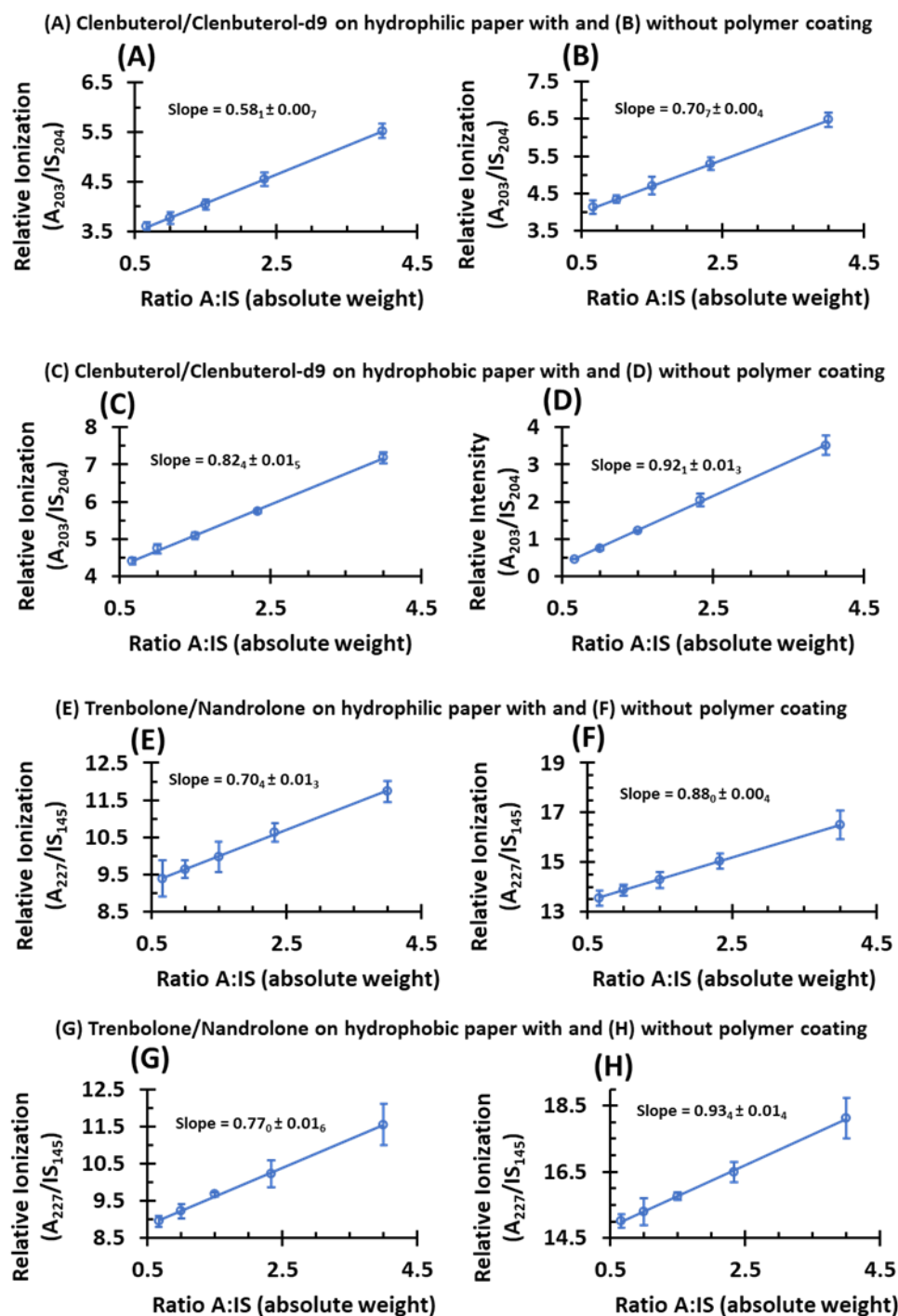


**Figure S11.** (A) Relative ionization efficiency curve for clenbuterol and clenbuterol-d9 in methanol on hydrophilic paper with polymer coating. The slope was determined to be  $0.581 \pm 0.007$ . (B) Relative ionization efficiency curve for clenbuterol and clenbuterol-d9 in methanol on hydrophilic paper without polymer coating. The slope was determined to be  $0.707 \pm 0.004$ . (C) Relative ionization efficiency curve for clenbuterol and clenbuterol-d9 in



methanol on hydrophobic paper with polymer coating. The slope was determined to be  $0.824 \pm 0.015$ . (D) Relative ionization efficiency curve for clenbuterol and clenbuterol-d9 in methanol on hydrophobic paper without polymer coating. The slope was determined to be  $0.920 \pm 0.013$ . (E) Relative ionization efficiency curve for trenbolone and nandrolone in acetonitrile on hydrophilic paper with polymer coating. The slope was determined to be  $0.704 \pm 0.013$ . (F) Relative ionization efficiency curve for trenbolone and nandrolone in acetonitrile on hydrophilic paper without polymer coating. The slope was determined to be  $0.880 \pm 0.004$ . (G) Relative ionization efficiency curve for trenbolone and nandrolone in acetonitrile on hydrophobic paper with polymer coating. The slope was determined to be  $0.770 \pm 0.016$ . (H) Relative ionization efficiency curve for trenbolone and nandrolone in acetonitrile on hydrophobic paper without polymer coating. The slope was determined to be  $0.934 \pm 0.014$ .

The percent difference was subsequently calculated from this study to determine if there was a difference in ionization efficiency due to competition of sample extraction from paper substrate and interactions with the polymer. A slight difference was observed in the coated samples relative to the non-coated samples, which likely stems from the inability to fully extract analytes from samples coated with polymer that is immiscible with organic solvents.

**Table S2.** Percent difference of relative ionization efficiencies of performance enhancing drugs in pure solution with and without polymer coating on paper substrate relative to matrix-free paper substrate.

Analyte	Percent Difference of Relative Ionization Efficiencies	
	Hydrophilic paper	Hydrophobic paper
Clenbuterol/clenbuterol-d9	18	10
Trenbolone/nandrolone	20	18

#### Matrix Effects of Dried Urine Spots on Paper Substrate

The impact of polymer coating on intrinsic matrix effects of urine samples was investigated using paper spray tandem mass spectrometry. The absolute intensity of clenbuterol and trenbolone in urine were measured against the absolute intensity observed in neat samples (i.e.,  $A_{\text{urine}}/A_{\text{neat}}$ ).

**Table S3.** Matrix effects of performance enhancing drugs spiked in urine and pure solutions on paper substrates relative to matrix-free paper substrate. The absolute signals of analyte were monitored via MS/MS.

Analyte	Matrix Effects of Urine Samples on Paper Substrate (%)			
	Hydrophilic paper		Hydrophobic paper	
	Non-coated	Coated	Non-coated	Coated
<b>Clenbuterol</b>	55	73	92	98
<b>Trenbolone</b>	55	71	82	92

#### References

- 1 P. A. Buxton, *Bull. Entomol. Res.*, 1931, **22**, 431–447.
- 2 P. A. Buxton and K. Mellanby, *BER*, 1934, **25**, 171.
- 3 D. E. Damon, M. Yin, D. M. Allen, Y. S. Maher, C. J. Tanny, S. Oyola-Reynoso, B. L. Smith, S. Maher, M. M. Thuo and A. K. Badu-Tawiah, *Anal. Chem.*, 2018, **90**, 9353–9358.